nature human behaviour

Article

https://doi.org/10.1038/s41562-026-02626-x

Multidimensional motor unit control after paralysing spinal cord injury using non-invasive recordings

Received: 22 December 2025

Accepted: 29 September 2026

Published online: 25 November 2026

Check for updates

Xingchen Yang[1,2,7], Vishal Rawji[2,3,4,7], Ciara Gibbs[2,7], Tianyu Jia[2], Lara Gouveia Vila[2], Agnese Grison[2], Ajoy Nair[5], Dario Farina[2,8] & Juan Alvaro Gallego[2,6,8]

Spinal cord injury results in profound motor impairment, which affects approximately 20 million people worldwide. Regaining hand use is one of their highest priorities. Interestingly, even severely affected individuals can still use spared connections to generate detectable activity (measured with electromyography) in their paralysed muscles when attempting to perform a movement. Here we asked whether participants with no hand function due to a cervical spinal cord injury could still control the activity of motor units from paralysed muscles, which we detected using high-density surface electromyographic recordings. Participants could readily control their motor units to accurately perform three different one-dimensional tracking tasks that imposed different control requirements, with performance plateauing after a few days of practice. Moreover, this accurate control readily transferred to a two-dimensional cursor navigation task, allowing participants to play a series of one-dimensional ('Pong') and two-dimensional ('Snake') games and to navigate a virtual wheelchair using three independent control signals. This robust performance was achieved despite the presence of spasticity, and even in one participant who had a motor complete injury. These findings demonstrate the promise of non-invasive motor unit recordings for restoring hand function and suggest potential avenues for rehabilitation after paralysis.

Spinal cord injury (SCI) affects approximately 20 million people worldwide, leading to major disability[1]. Loss of hand function profoundly reduces independence and quality of life; consequently, tetraplegic individuals with SCI highly prioritize its recovery[2].

Advances in invasive techniques to stimulate the spinal cord[3], nerves[4] or muscles[5–7] show promising results for restoration of volitional control of the hand by building on residual connections and creating new ones, while intracortical brain–computer interfaces[8–10] (BCIs) hold potential for functional compensation by mapping cortical activity onto signals to control external devices. Yet, in both cases, the need for surgery limits their accessibility[11]. Here we explore a non-invasive alternative for functional compensation of lost hand function.

Even following a complete lesion that prevents any overt movement, residual connections remain between motor regions in the brain and spinal motoneurons below the injury[12]. As a result, it is possible to detect the residual muscle activity using electromyography (EMG) with

[1]School of Automation, Southeast University, Nanjing, China. [2]Department of Bioengineering, Imperial College London, London, UK. [3]King's College London, London, UK. [4]King's College Hospital, London, UK. [5]Alderbourne and Daniels Rehabilitation Unit, Hillingdon Hospital, London, UK. [6]Neuroscience of Disease Programme, Centre for Restorative Neurotechnology, Champalimaud Foundation, Lisbon, Portugal. [7]These authors contributed equally: Xingchen Yang, Vishal Rawji, Ciara Gibbs. [8]These authors jointly supervised this work: Dario Farina, Juan Alvaro Gallego. e-mail: d.farina@imperial.ac.uk; juan.gallego@research.fchampalimaud.org

Table 1 | Participant characteristics

Participant	Age	Gender	Level	ASIA[a]	Tested hand	Upper limb MRC power of tested arm[b]	Duration of injury (months)	Experiment time (months)	Sensory deficit
P1	30s	Male	C4	C	L	0–1 in hand and wrist[c]	24	9	Loss of pinprick
P2	60s	Male	C1–C3	C	R	0 in hand and wrist[d]	14	9.5	Complete loss below shoulders
P3	50s	Male	C2–C4	A	R	0–1 in hand and wrist	12	6	Minimal to complete loss below shoulders

[a]This scale measures the severity of SCI and includes measurement of sensory and motor function. ASIA A, complete injury; ASIA B, sensory but not motor function; ASIA C, motor incomplete. [b]The MRC grading scale tests power. Results here report MRC-graded power in the wrist and hand. 0, no movement; 1, flicker of contraction; 2, active movement with gravity eliminated; 3, active movement against gravity; 4, active movement against resistance; 5, normal power. [c]Except wrist extension, 3/5. [d]Except ring extension, 1/5.

surface electrodes[13,14]. Previous work provides evidence that people with an incomplete SCI can use these residual EMG signals to control computer cursors[15] and assistive devices[16,17]. However, surface EMG signals from paralysed muscles have inherent limitations that prevent accurate control. First, since the injury deprives many motoneurons of their inputs, surface EMG signals in people with SCI only reflect the activity of a limited number of motor units (a motoneuron and the fibres it innervates) resulting in a low signal-to-noise ratio (SNR). This makes surface EMG signals unreliable as control signals[18]. Second, for the up to 70% of SCI survivors suffering from spasticity[19,20], the surface EMG signal becomes unusable due to the tonic firing of many of the remaining motor units[21,22]. This would leave many people unable to benefit from this type of technology.

Paradoxically, control based on the activity of a few single motor units, rather than the 'global' EMG, could overcome these limitations. First, motor unit action potentials are discrete events that can be counted to extract continuous control signals, such as those in intracortical BCIs[8,9]. Second, in people with spasticity, motor units that exhibit tonic firing could be excluded as control signals, retaining only those units that can be voluntarily modulated. Building on observations that single motor unit activity can be detected from surface EMG recordings in people with SCI[13,14], enabling tracking of simple profiles[13,23] and offline classification of attempted movements[24], we hypothesized that individuals with SCI can achieve proficient control of motor unit populations from paralysed muscles.

We investigated the control performance, potential for improvement and dimensionality of motor unit control in three people with no functional use of their hand(s) due to cervical SCI. Even if they exhibited, at most, minimal flickers of muscle contraction during attempted movements, all participants could readily control the activity of motor units from affected muscles to accurately track three different one-dimensional profiles, even in the presence of prominent spasticity. This control improved during the first days of practice, with performance plateauing before five sessions. Participants could readily extend this control to a second and even a third degree of freedom, with minimal degradation in control performance. This robust control allowed them to play adapted versions of the games 'Pong' (one degree of freedom) and 'Snake' (two degrees of freedom), and, in a step towards functional applications, navigate a virtual wheelchair using three degrees of freedom. Our work establishes a proof of concept that supports the development of motor-unit-based assistive devices and gamified therapies for people with paralysis.

Results

Experimental paradigm

Three males (in their 30s, 60s and 50s, referred to as P1, P2 and P3) who suffered from an SCI ranging from the C1 to C4 level participated in this study. None had any functional movements in their tested hand, with Medical Research Council (MRC) power ranging from 0 (no movement) to 1 (flicker of movement). Participant characteristics are summarized in Table 1 (see Methods for further details).

First, in a screening session, we instructed the participants to attempt various finger or wrist movements while recording high-density surface EMG (HDsEMG) signals from their forearms using three 64-electrode arrays (8 × 8; inter-electrode distance, 10 mm) (Fig. 1). On the basis of this screening, we selected for each participant one attempted movement that elicited discernible EMG but minimal observable movement, which they then used for the one-dimensional control experiments. The selected attempted movements were thumb adduction, wrist abduction and wrist abduction for P1, P2 and P3, respectively (for example, Supplementary Video 1).

To detect the activity of single motor units, at the beginning of each session we recorded HDsEMG signals as participants performed and sustained their selected attempted movement by controlling the global EMG amplitude to track a trapezoidal profile. We then used validated blind-source separation techniques[25,26] to isolate the activity of single motor units from these HDsEMG recordings. For the online experiments, we applied the motor unit filters obtained through offline blind-source separation to the HDsEMG data in real time, an approach that we validated offline (Supplementary Fig. 1a,b). This allowed us to first visualize the spiking of the detected motor units as participants attempted their selected movements, and to then map them onto control signals for the online control experiments. Overall, we detected an average of 6.9 ± 3.1 (mean ± s.d.; range, 2–12) motor units for the attempted movement across all participants and sessions.

Motor units could be classified into one of two distinct categories based on their online firing behaviour: controllable (62.5% of the units across all the recordings) and tonic (37.5%) (examples in Fig. 2a and Supplementary Fig. 1c,d), the proportion of which differed between participants and between sessions (Supplementary Fig. 2a). Controllable motor units were characterized by activity exclusively during movement attempts, while tonic motor units fired continuously during both rest and movement attempts, probably due to underlying spasticity[21,22]. Controllable units only rarely exhibited tonic activity, and this change was transient (6.06% ± 5.6% of all units across all participants and training sessions; Supplementary Fig. 2b,c), suggesting underlying physiological changes in tonic motor unit properties related to this behaviour[27,28]. Our prediction was that participants would be able to perform the tasks well using controllable motor units, even in the presence of tonically firing units.

Motor unit activity enables accurate and proportional control across different one-dimensional tasks

We investigated whether participants could harness the activity of identified motor units for precise continuous control by asking them to control the vertical position of a cursor. We designed three types of target profiles, each imposing a different control requirement (Fig. 2b): a trapezoidal profile, which required maintaining the control signal at a constant level, similar to holding a posture; a sinusoidal profile, which

https://doi.org/10.1038/s41562-026-02626-x

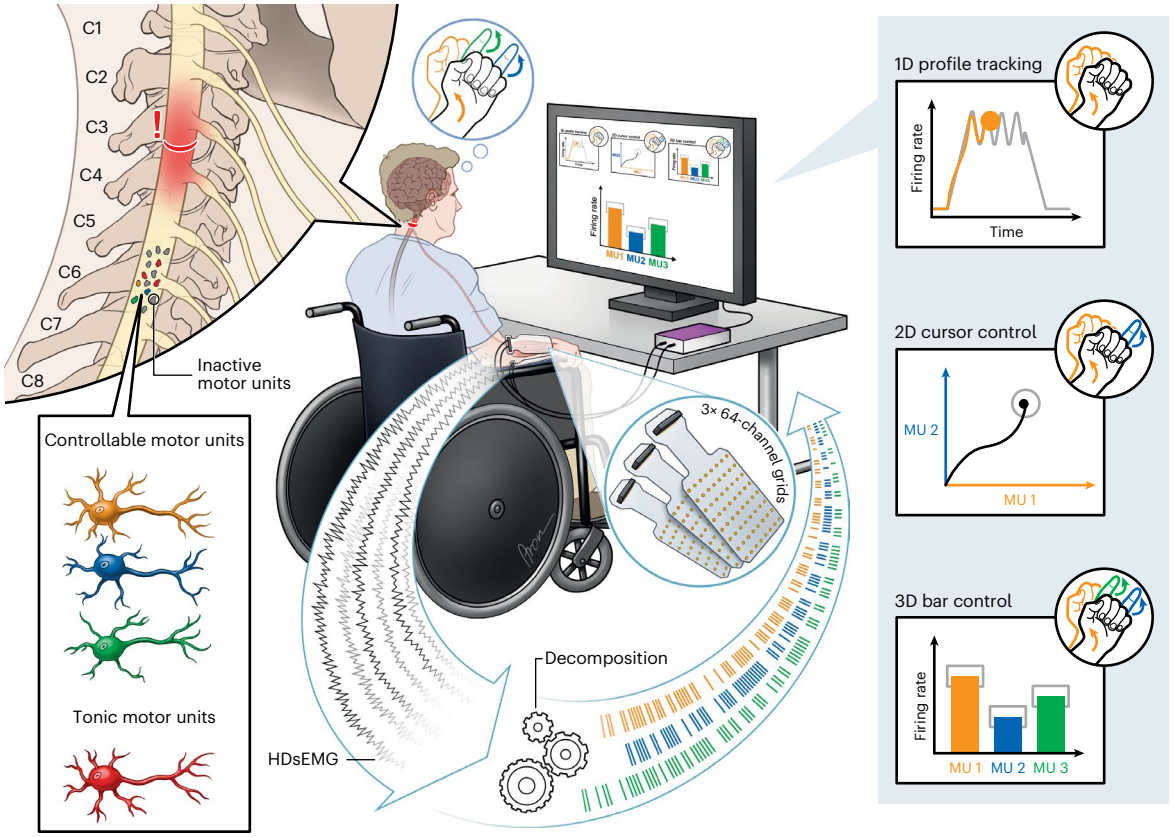


Fig. 1 | Investigating motor unit control in individuals with no hand function following a cervical SCI. Motor unit (MU) activity was detected through decomposition of HDsEMG recordings. We detected both 'controllable motor units' that participants could modulate voluntarily and 'tonic motor units' that were not under volitional control, probably due to spasticity. Each colour (orange, blue and green) represents a different motor unit that could be independently controlled. Participants achieved flexible control for one-dimensional profile tracking, two-dimensional cursor control and three-dimensional control of three different bars. This control was also extended to two different games and simulated wheelchair navigation using three independent control signals. Credit: illustration by Aron Cserveny.

required smooth and predictable modulation; and a pseudosinusoidal profile, which demanded flexible control of both timing and intensity. For motor-unit-based control, we tested both the participant's ability to modulate the firing rate of a single motor unit and of a population of motor units associated with the same attempted movement—often referred to as a cumulative spike train[29]—to better capture the overall behaviour of all active spinal motoneurons in a pool[30]. To test our prediction that motor unit activity should provide better control than the global EMG, participants also repeated all the profiles using the global EMG amplitude as a control signal. This 3 × 3 design (control signals × profile types) resulted in nine unique trial types, the order of which was randomized (Methods). Participants performed three repetitions of each trial type in each session.

All participants achieved stable proportional control across the three target profiles from the first session (Fig. 2b, Supplementary Fig. 3 and Supplementary Video 1). For P1 and P2, control based on a population of motor units yielded the highest accuracy, followed by single motor unit control, and EMG-based control performed the worst (Fig. 2b and Supplementary Fig. 3a). For P3, EMG-based control was as accurate as that for a population of motor units in the trapezoidal and sinusoidal profiles and performed best in the pseudosinusoidal profile (Supplementary Fig. 3b); we attributed this to his surface EMG being relatively sparse and thus strongly resembling the detected motor unit population, as shown by the high correlation between these two signals (Supplementary Fig. 4a,b). P3's EMG SNR was also the highest of all three participants (Supplementary Fig. 4c). However, overall, control of a population of motor units demonstrated high accuracy, outperforming all other modalities in virtually all comparisons. This improved control was in part related to excluding tonic units, as shown by our offline simulations (Supplementary Fig. 4d). Finally, this accurate control was not driven by overt movements, as demonstrated by the very low correlation (<0.3) between pooled motor unit activity and any flickers of movement (Supplementary Fig. 5).

Proportional, accurate motor unit control is possible from day one, improving only modestly with practice

We next assessed whether participants could improve their control with practice. Participants tracked the three profiles using motor units associated with the same attempted movement for four to five sessions spanning a period of 4 to 12 weeks (examples in Fig. 3a). We noted a modest improvement in tracking accuracy that plateaued by the third or fourth session (Fig. 3b, Supplementary Fig. 6a–c and Supplementary Table 1). This improvement was not related to an increase in the number of motor units over sessions, which did not change significantly over time (Supplementary Fig. 2a), and happened despite the participants only occasionally controlling the same motor units in different sessions (Supplementary Fig. 6d,e). Together, these observations suggest that the performance gains stemmed from increased familiarity with the control. Importantly, these performance gains seemed to hold over time: we tested P1 for retention by having him repeat both forms of motor unit control more than 60 days after his last practice session and found that tracking performance remained comparable to the final—not the first—practice session (Supplementary Fig. 7).

We hypothesized that tracking was accurate from the first session and improved little with practice because participants controlled motor units by attempting movements they already knew—how to

https://doi.org/10.1038/s41562-026-02626-x

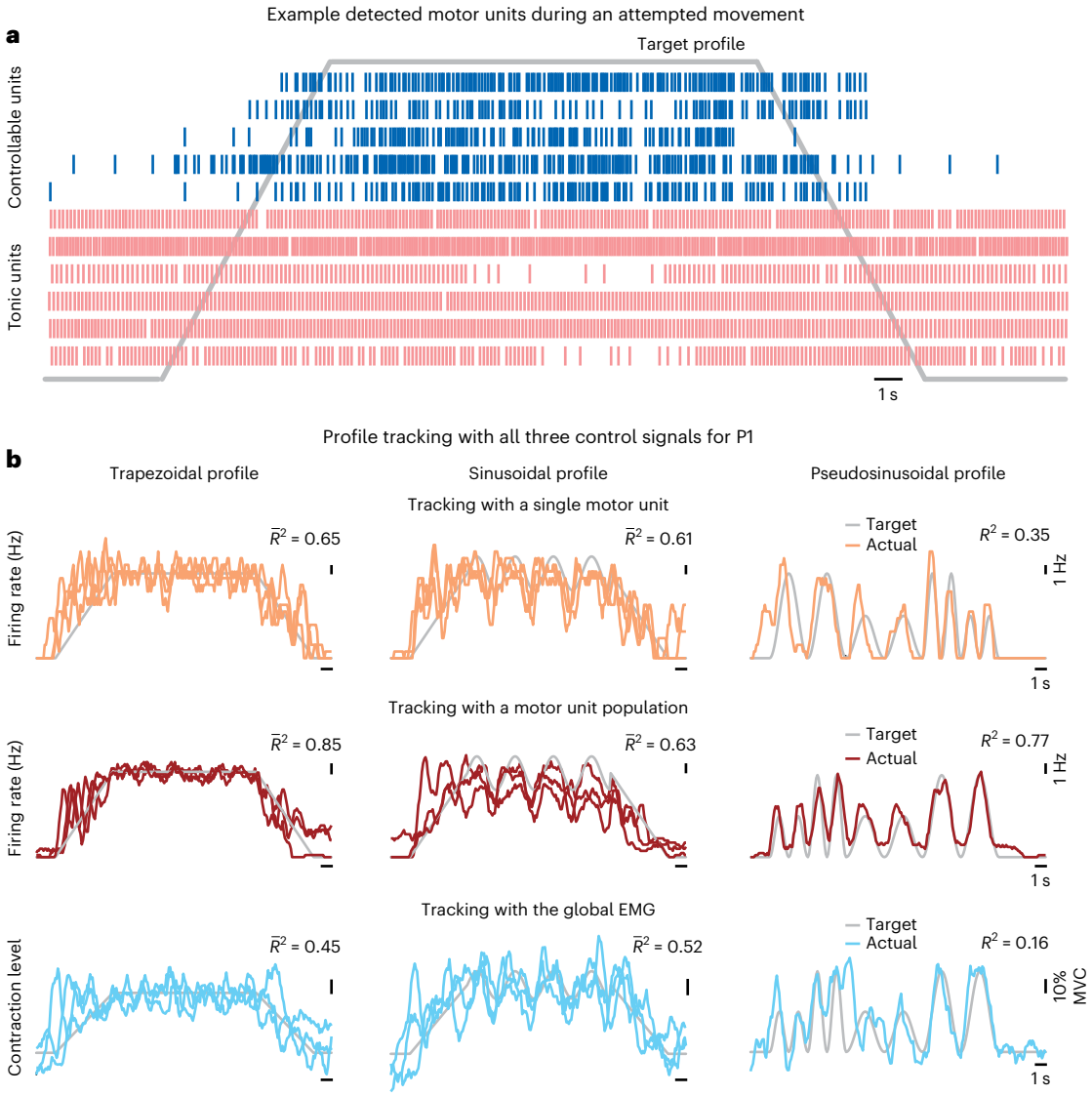


Fig. 2 | Accurate motor unit control on the first day. a, An example of detected motor unit activity, showing a representative combination of controllable units, whose activity could be volitionally modulated (dark blue), and tonically active units probably related to spasticity (light red). Data from P1. **b**, Online control for the first session from P1 as he tracked the three profiles using the activity of a single motor unit, a population of motor units or the global EMG. Tracking accuracy was measured with the coefficient of determination (R^2); $\bar{R}^2$ is the average tracking accuracy across multiple trials. Each pseudosinusoidal trial was unique, so only one trial is presented for clarity. Tracking for P2 and P3 is shown in Supplementary Fig. 3.

perform, engaging spared connections from the same neural pathways that produced those movements before injury. That is, participants were controlling the attempted movement rather than the motor unit directly. To test this notion, we assessed the control performance from motor units associated with attempted movements that did not undergo repeated practice (termed 'untrained movements'): wrist flexion for P1 and little finger extension for P3; we were unable to test P2 due to time constraints. Consistent with the view that motor unit control arose from already known movements, participants could also accurately control motor units associated with these untrained attempted movements, with almost comparable performance to the trained movements, even on their first session (Fig. 4).

Flexible two-dimensional and three-dimensional control using multiple independent motor units

Meaningful functional restoration demands more sophisticated control than the one-dimensional control described above. We therefore investigated the feasibility of controlling two independent motor units for cursor navigation in a two-dimensional workspace, akin to the way participants would interact with a tablet or computer. We instructed the participants to select two different attempted movements and use one motor unit associated with each of them to move the cursor along the horizontal and vertical axes, respectively. P1 selected thumb adduction and wrist abduction; P2, wrist abduction and ring extension; and P3, thumb flexion and little finger extension. Then, in an initial calibration phase, we verified that the selected motor units could be activated independently (Methods).

Participants demonstrated competent two-dimensional cursor control immediately, being able to acquire 16 different targets per block and hold the cursor for >375 ms (Fig. 5a,b and Supplementary Video 2). Overall success rates were 85%, 96.25% and 92.5% for P1, P2 and P3, respectively, with an average time to success of 2.74 s, 4.08 s and 4.67 s. Participants could easily acquire targets along either the horizontal or vertical axis, confirming their ability to independently control these motor units (Fig. 5a). Off-axis targets were slightly more difficult to acquire, as shown by their lower success rate, longer times to completion and lower 'path efficiency' (that is, the produced trajectories deviated more from the optimal straight-line trajectory, leading

https://doi.org/10.1038/s41562-026-02626-x

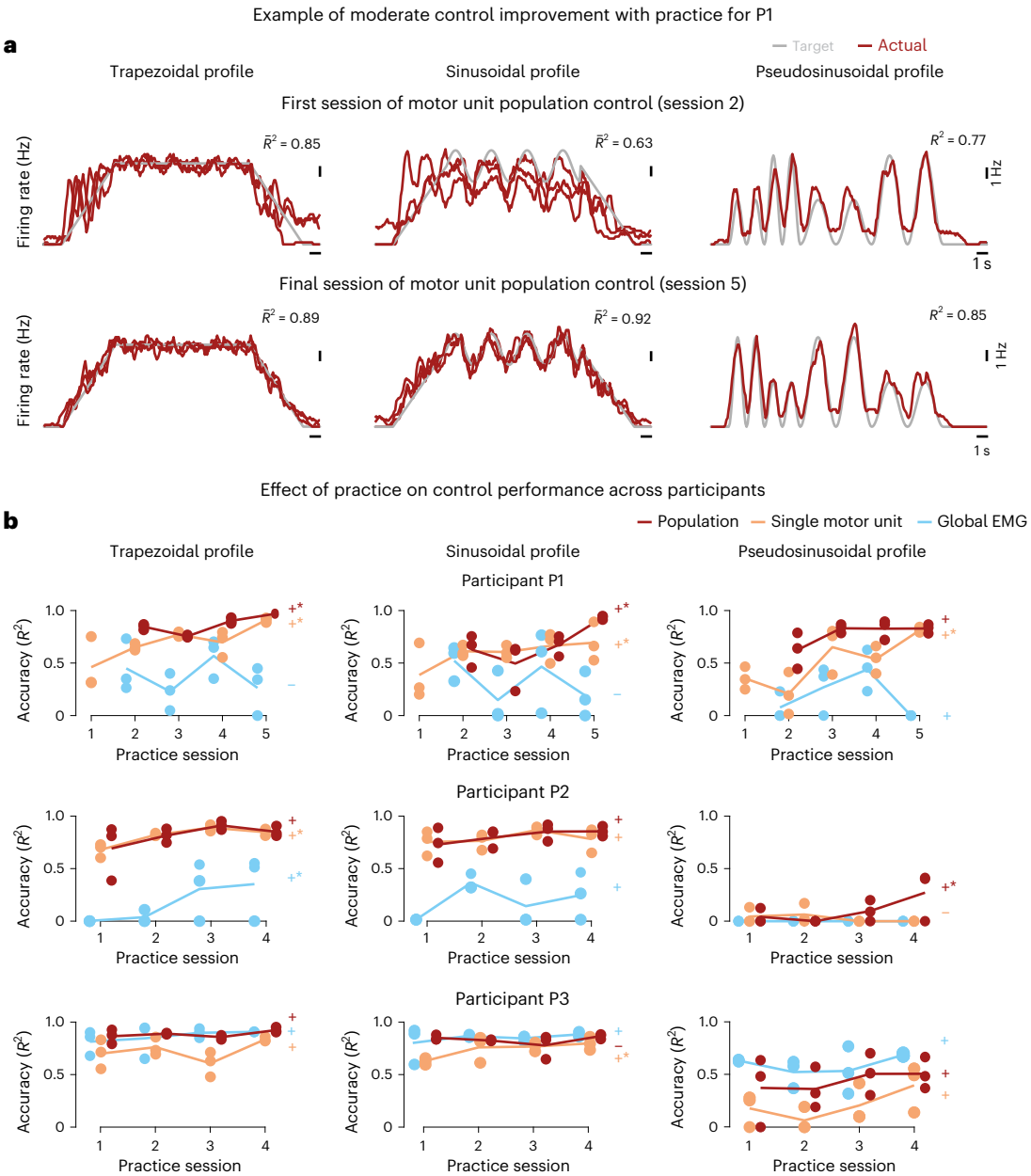


Fig. 3 | Motor unit control improves only modestly over practice sessions. **a**, Example tracking for all three profiles and control signals for the first and last session with P1. **b**, Tracking performance across practice sessions spanning 4 to 12 weeks for all three participants. For P1, EMG and motor unit population control started from the second session. We fitted linear regressors to the across-day performance trends; a plus sign indicates a positive slope, a minus sign indicates a negative slope, no sign indicates a zero slope and an asterisk indicates a statistically significant change (*$P < 0.05$, two-sided t-test). These symbols are colour-matched with the control signals.

to values further away from 100%) (Fig. 5c). Closer inspection of individual trials showed that participants used a mixture of two different strategies to reach these off-axis targets: simultaneous co-activation of both motor units and sequential individual activation of one motor unit and then the other (Fig. 5a and Supplementary Fig. 8a). Participants used each of these strategies to varying degrees both between and within trials (Supplementary Fig. 8b), independent of the distance to the target (Supplementary Fig. 8c). Overall, greater co-activation was associated with longer completion times, whereas the use of individual, sequential motor unit control was associated with shorter completion times (Supplementary Fig. 8d). Finally, two-dimensional motor unit control was robust: for example, one participant exhibited myoclonic jerks that transiently hindered his control (Fig. 5a, in blue), but could regain it immediately after and complete the trial.

Our two-dimensional control task design incorporated asymmetrical training histories: one motor unit was associated with an attempted movement that participants had extensively practised during one-dimensional control (Fig. 3), while the other corresponded to a novel, untrained attempted movement. On the basis of our observation of similarly accurate one-dimensional control for motor units associated with attempted trained and untrained movements (Fig. 4), we also expected two-dimensional control performance to be similar across 'trained' and 'untrained' motor units. Indeed, performance for targets on either the horizontal or vertical axis, which required the independent activation of the trained or untrained motor units, showed no significant difference for time to completion (two-sided Mann–Whitney U-test, P1, $U = 106$, $P = 0.787$; P2, $U = 84.5$, $P = 0.245$) and path efficiency (two-sided Mann–Whitney

https://doi.org/10.1038/s41562-026-02626-x

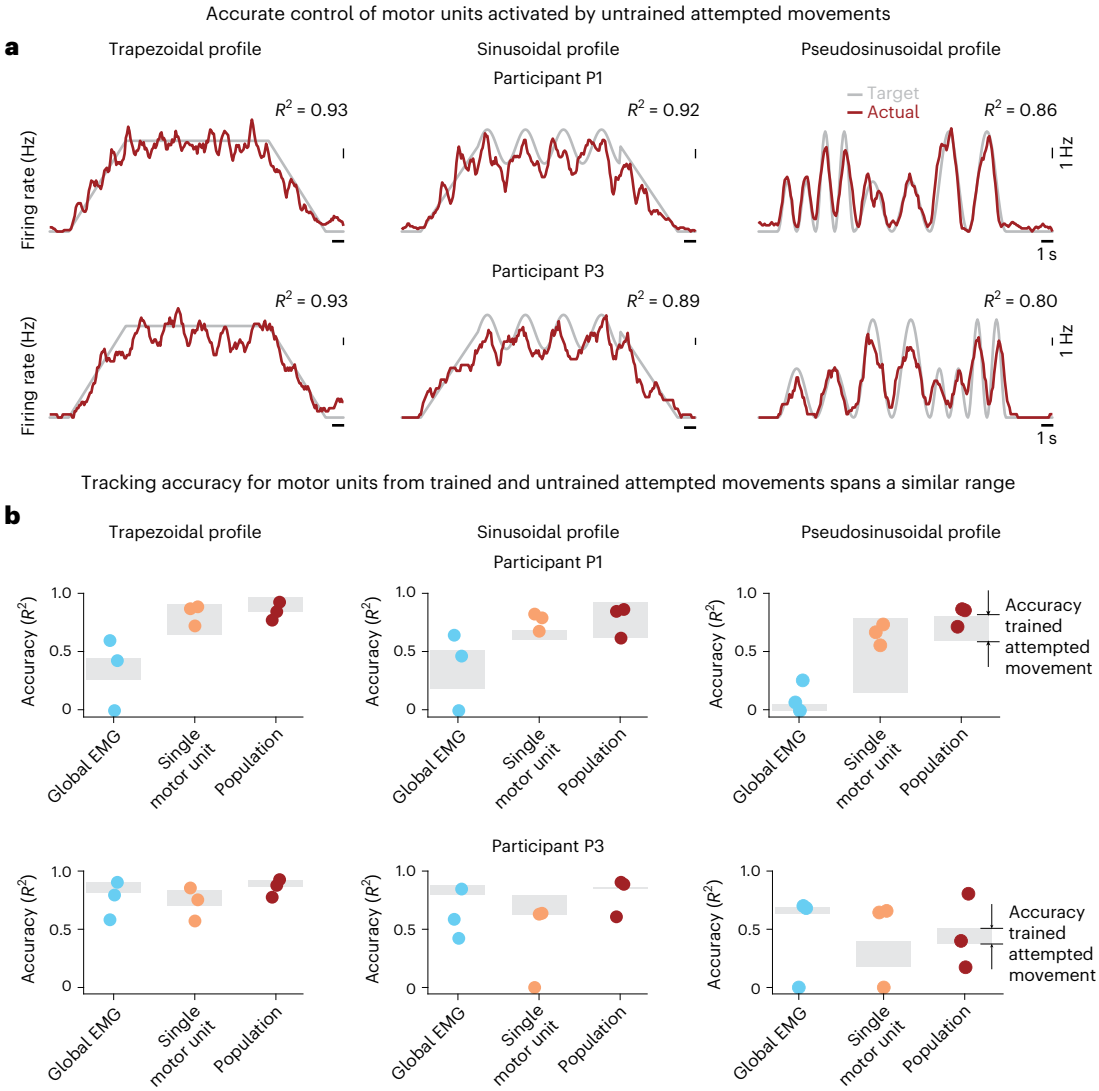


Fig. 4 | Accurate control with motor units associated with untrained attempted movements. a, Example tracking for all three profiles and control signals for untrained attempted movements for the last sessions with P1 and P3 (the first session in which they attempted control using untrained attempted movements). **b**, Comparison of tracking performance for trained and untrained attempted movements. Untrained movements were tested for three sessions; participants completed one trial per session for each tracking condition (coloured circles). The grey rectangles show tracking performance for trained movements. Bottom: tracking accuracy on the first session; top: tracking accuracy on the last session. Note that performance for trained and untrained spans a similar range for most comparisons.

U-test, P1, $U = 90$, $P = 0.351$; two-sided *t*-test, P2, $t_{28} = -1.25$, $P = 0.223$) (Fig. 5d,e). Finally, having observed similarly accurate control for trained and untrained motor units, we tested the prediction that two-dimensional control would already be at near-maximal performance from the first session and would not improve with practice. As expected, P1 showed no clear performance gains after four sessions (Fig. 5f). Likewise, P2 performed roughly as well as in the first experiments when he used motor units associated with two different untrained attempted movements (thumb extension and wrist extension) for two-dimensional cursor navigation nine months after his last experimental session (success rate, 95%; average time to success, 6.94 s) (Supplementary Fig. 9).

Can participants control more degrees of freedom using motor units from paralysed hand and wrist muscles? To answer this, we explored three-dimensional control in P1 and P2 using a 'three bars' task (P3 was not tested due to time constraints). After a motor unit selection procedure similar to that used for two-dimensional control, P1 selected motor units associated with attempted thumb adduction, wrist abduction and wrist flexion, and P2 those associated with wrist abduction, ring extension and index extension. Both participants successfully achieved independent, proportional, real-time control over three motor units (Supplementary Video 3). This control again demonstrated notable flexibility: P1 adeptly performed the two-dimensional cursor control task using all possible pairwise combinations of the three independent motor units (Fig. 6a). Both participants were also able to selectively activate one motor unit to a target level while keeping the other two quiescent (Fig. 6b,c), but found simultaneous co-activation of multiple motor units more difficult (Fig. 6d,e), reminiscent of difficulties with co-activation during two-dimensional control (Supplementary Fig. 8). Combined, these results show that although the simultaneous control of multiple motor units is challenging, people with severe paralysis resulting from a cervical SCI can control multiple independent motor units from wrist and hand muscles with minimal practice.

Applications to gaming and assistive devices

We have so far focused on laboratory tasks designed to understand the ability of SCI participants to control the activity of motor units

https://doi.org/10.1038/s41562-026-02626-x

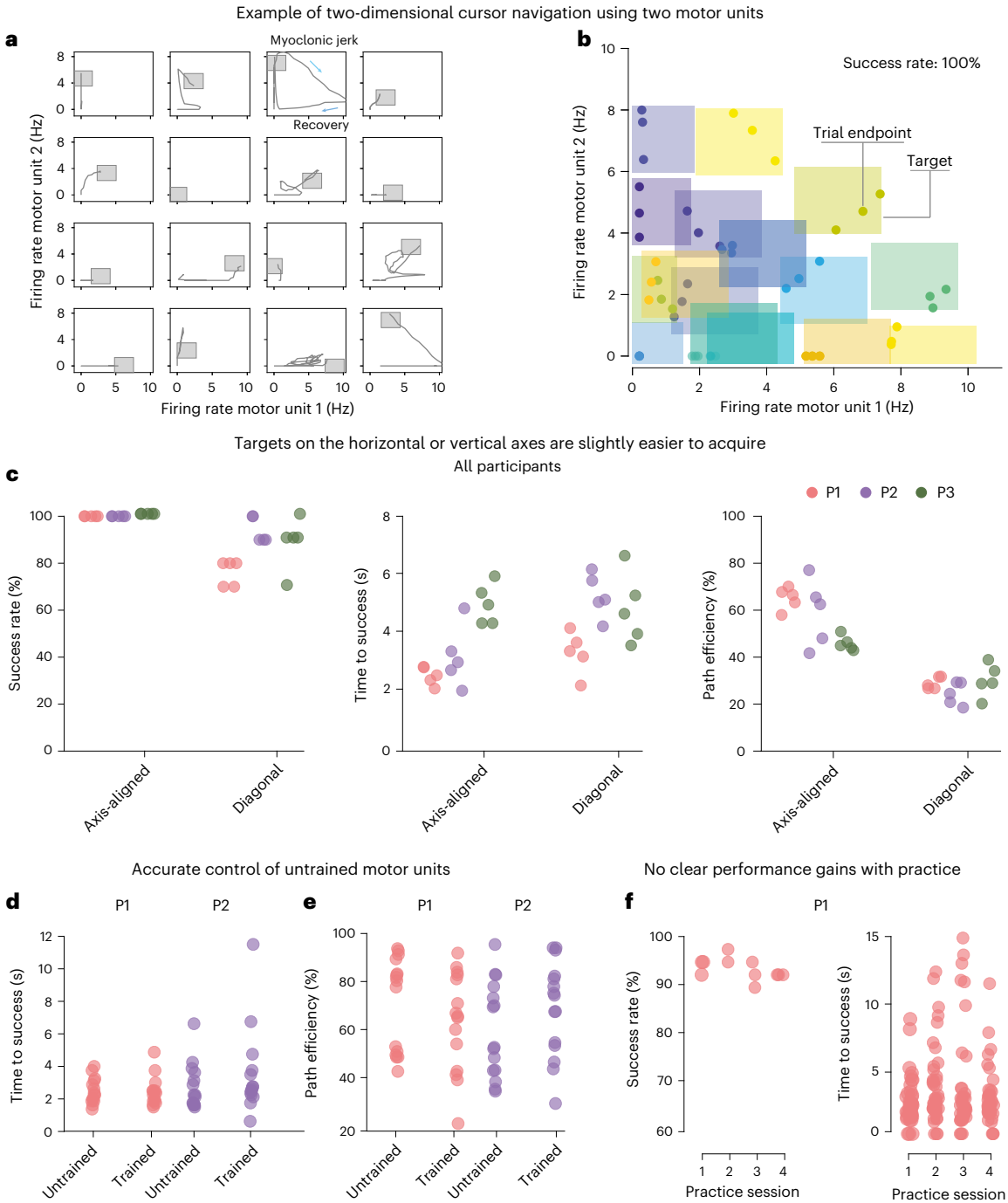


Fig. 5 | Two-dimensional cursor navigation using two independent motor units. a, Example cursor trajectories for 16 trials from the same session with P3. Note that during one of these trials the participant suffered a myoclonic jerk but recovered control quickly (shown with blue arrows). **b**, Example targets (coloured rectangles) and cursor positions (coloured circles) at the end of the hold period for all the trials from one session with P3. **c**, Performance (success rate, time to completion and path efficiency) for axis-aligned versus off-axis targets for each participant. **d**,**e**, Time to completion (**d**) and path efficiency (**e**) were not significantly different for trained and untrained movements. $P > 0.05$, two-sided Mann–Whitney *U*-test. **f**. Control performance over four sessions of practice with P1 shows no strong trend.

from paralysed muscles. Successful deployment of this technology for assistive devices or even rehabilitation could benefit from extensive practice well beyond the relatively limited number of sessions that we have explored here. As a first step towards more engaging, gamified training, we developed adapted versions of Pong[31] and Snake[32]. P2 and P3 played Pong, controlling the vertical movement of the paddle by modulating the firing rate of either a single motor unit or a population of motor units (Fig. 7a and Supplementary Video 4). P1 and P3 played Snake, where the activation of one motor unit made the snake turn 90° clockwise, and the activation of another, 90° counterclockwise (Fig. 7b and Supplementary Video 5). All participants demonstrated proficient control after an initial familiarization period, although, for Snake, both participants cited difficulties with directional orientation, as the snake's turning mechanics varied based on its current trajectory.

In a step towards controlling an assistive device, we asked P1 to navigate a virtual wheelchair using the activity of three motor units (Fig. 7c), where one motor unit controlled the forward movement, and the other two the left and right turns. P1 could immediately navigate

https://doi.org/10.1038/s41562-026-02626-x

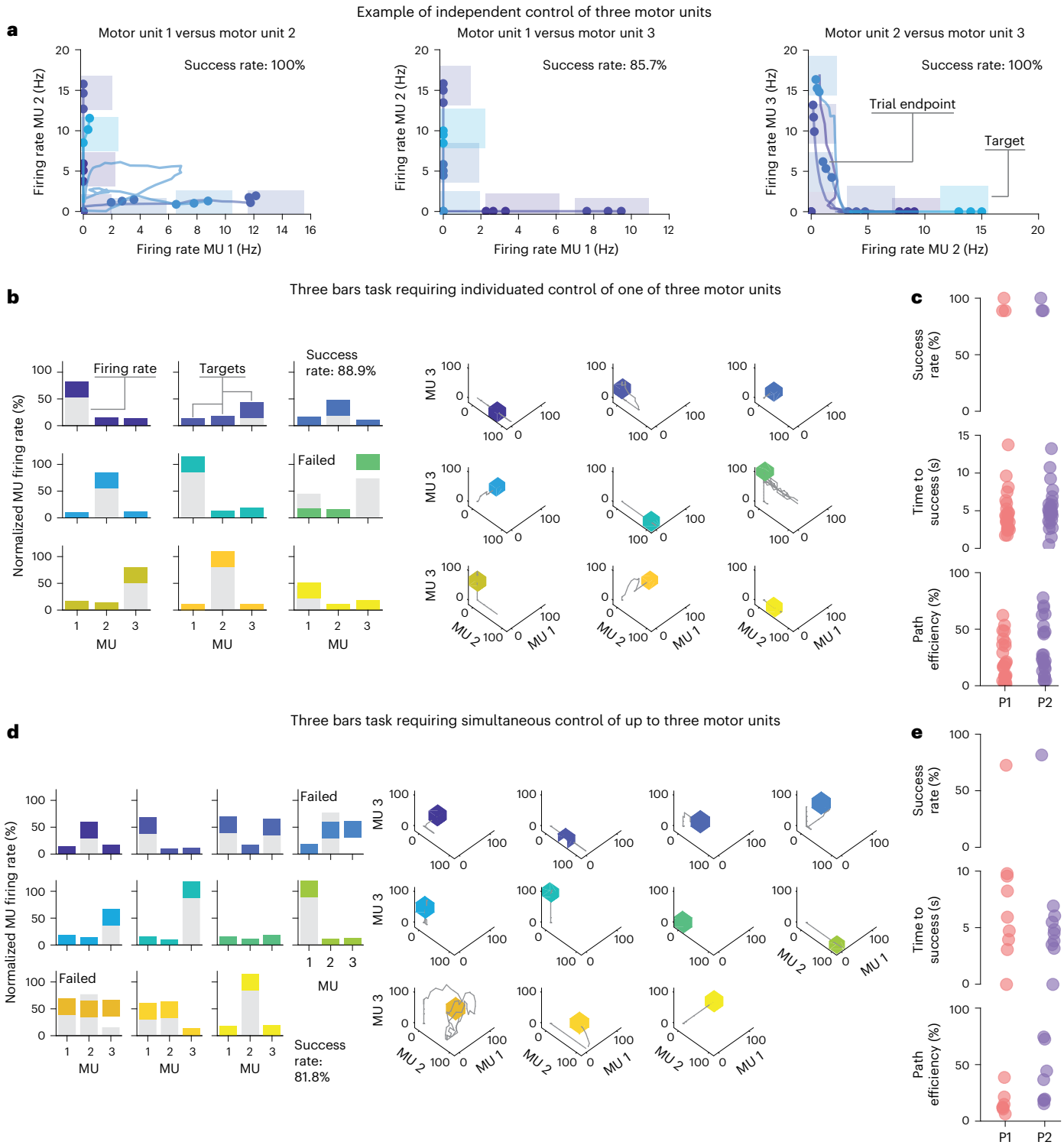


Fig. 6 | Independent and simultaneous control of three motor units. a, Each plot shows independent motor unit activation with different combinations of three different motor units in the two-dimensional control task in one session with P1. **b**, Example trials from a three bars task that required isolated activation of one of three motor units. The coloured rectangles indicate target firing rates, and the grey bars indicate actual firing rates. The right panel shows control trajectories in a three-dimensional normalized firing rate space. Firing rates were normalized for visualization. Data from P1. **c**, Performance metrics across all sessions for the task in **b**. **d**, Similar to **b**, but for a version of the three bars task that required simultaneous activation of multiple motor units in four trials per session. Data from P2. **e**, Performance metrics across all sessions for the task in **d**.

the wheelchair along the path (Fig. 7c). Importantly, all participants expressed enthusiasm about using their residual motor unit activity for gameplay and virtual wheelchair control. This positive feedback underscores the potential of this technology to provide both engaging, recreational experiences and effective assistance for individuals with SCI.

Discussion

We have demonstrated that individuals with no hand function following cervical SCI can harness the activity of motor units from paralysed muscles to achieve proportional, continuous and multidimensional control despite the lack of overt movement. Importantly, the controlled

https://doi.org/10.1038/s41562-026-02626-x

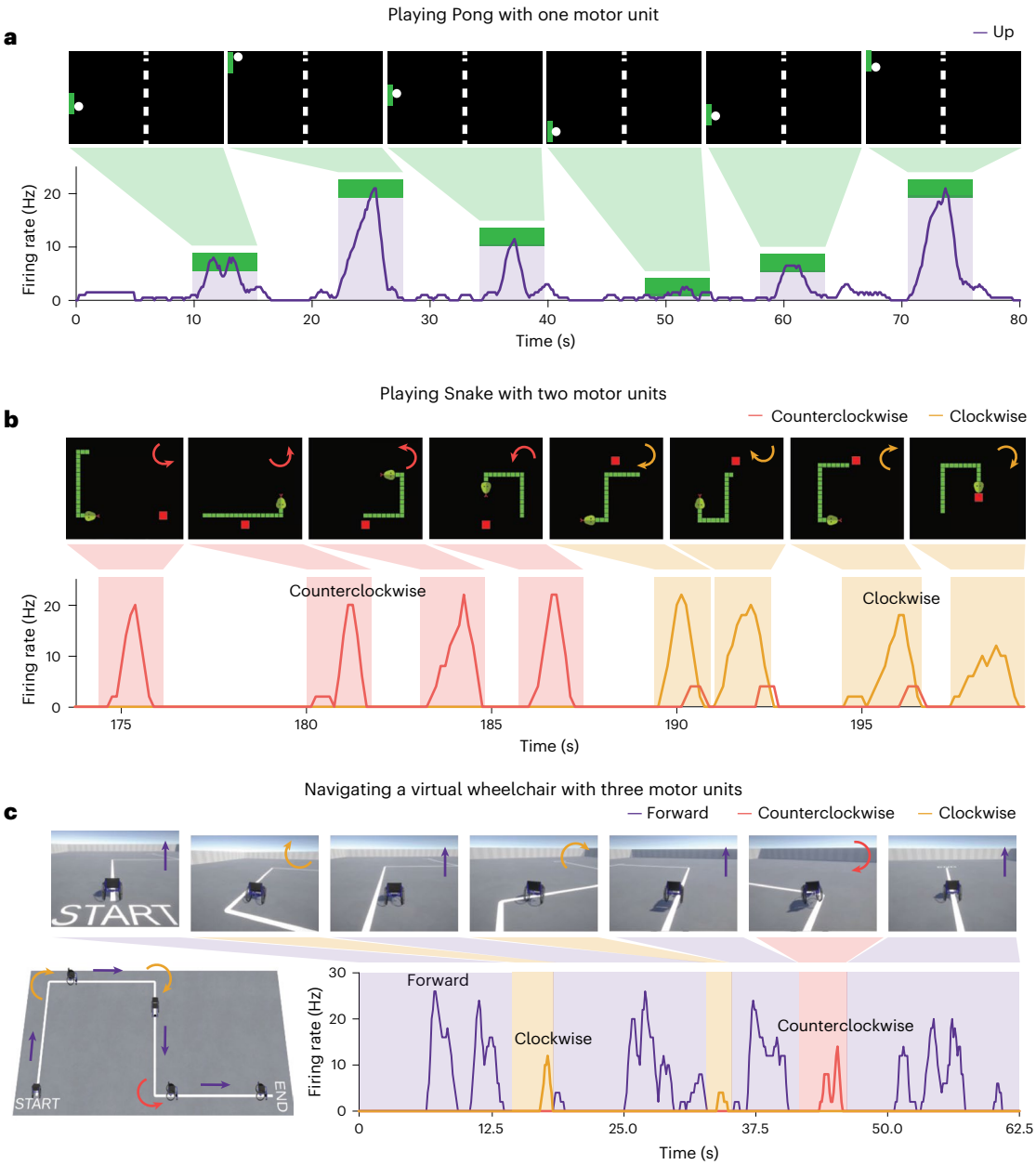


Fig. 7 | Playing games and controlling a virtual wheelchair using the activity of up to three motor units. a, Playing Pong with one motor unit. Top: position of the paddle and the ball during 80 s of play; bottom: firing rate of the motor unit controlling the paddle position. The purple trace indicates the motor unit firing rate; the green rectangles indicate the position of the paddle. **b**, Playing Snake with two motor units. Participants had to bring the snake (in green) to its food (in red). Top: example position of the snake and the food during ~25 s of play; bottom: firing rate of the two motor units used for control. **c**, Independent control of three motor units to drive a virtual wheelchair along a target path towards a goal location. Top: example screenshots during a trial; bottom left: target trajectory and example positions of the virtual wheelchair for one example trial; bottom right, activation of the three motor units controlling the different actions.

motor units were detected non-invasively through the decomposition of HDsEMG recordings[25,26,33], which we could accomplish even for a participant classified as motor complete and for others who exhibited clinical signs of spasticity. These findings have direct implications for the development of motor-unit-based assistive technologies and may inspire future rehabilitation interventions for paralysis caused by disorders such as SCI[34] and stroke[35,36].

Motor unit control is accurate because it builds on attempted movements

All three participants showed good one-dimensional control from the outset (Fig. 2b and Supplementary Fig. 3), with only small gains following several sessions of practice (Fig. 3 and Supplementary Fig. 6a–c). We believe this happened because controlling motor units by attempting specific movements engaged descending inputs from brain structures that were naturally involved in hand control and remained unaltered despite the lesion[37]. Consistent with this view, controlling motor units associated with attempted movements that participants had not explicitly trained for was as accurate from the outset as controlling motor units associated with attempted movements that participants had trained for over several days (Fig. 4), and participants retested after two (Supplementary Fig. 7) or even nine months (Supplementary Fig. 9) showed no performance loss. This immediately accurate control contrasts with 'neurofeedback paradigms' requiring

extensive training[38–40] and supports the application of motor unit control for assistive devices.

Even if participants could readily expand their accurate control to two or three degrees of freedom, our work reveals looming challenges. During cursor navigation in a two-dimensional workspace, targets off the horizontal and vertical axes, which required co-activation, were more difficult to reach (Fig. 5c). Indeed, participants reached these off-axis targets by alternating between two strategies: simultaneous co-activation of the two units, and sequential, individual activation of one unit and then the other (Supplementary Fig. 8). The greater difficulty to co-activate may be because the combination of attempted movements was often unnatural (for example, thumb flexion and little finger extension for P3), and hence it may have been difficult to control the attempted contraction of those muscles simultaneously[41]. In future work, we will select movements that are naturally co-occurring and whose motor units are therefore more intuitively co-activated.

We noted that some participants had difficulty holding the cursor at a particular location for long periods of time (Fig. 5a and Supplementary Figs. 8a and 9a). An interesting way to simplify this problem would be to change the nature of the mapping between the motor unit firing rate and cursor behaviour. For instance, instead of using position mapping, we could use velocity mapping, as is often done in intracortical BCIs[42,43]. Mappings based on Kalman filters[44] or machine learning techniques[45,46], as well as shared human–machine control approaches[39], are other ways to potentially make control easier for the user. Even simple optimization of the scaling of the control mapping could lead to important improvements in the usability beyond the proof of concept provided in this study.

EMG decomposition into constituent motor units improves control

Isolating the activity of single motor units improved control relative to the global surface EMG by enhancing the fidelity of the control signal. This was due to two reasons. First, surface EMG is affected by non-physiological factors[47] such as changes in skin conductance[48] (for example, due to sweat) and electrode displacement. These factors result in surface EMG signals that vary over time, thus requiring recalibration to prevent unstable control (3.7 ± 1.6 times per session; range, 1–6). In contrast, HDsEMG decomposition largely filters out these non-physiological factors, inherently making motor unit control more robust. Second, we could exclude unwanted motor units from the control signals, which proved crucial due to the presence of a large number of tonically active motor units (~35%; Supplementary Fig. 2a), probably due to spasticity[21,22], that our simulations suggested would have dramatically hindered control (Supplementary Fig. 4d). Such filtering is not possible for the global EMG[47], since it reflects the summed contributions of all motor units indiscriminately[49]. Crucially, offline decomposition alone was not enough to classify motor units as tonically firing or controllable; only real-time tracking confirmed which neurons were under voluntary control.

While control based on both populations of motor units and single motor units was very accurate, even without any additional postprocessing[50], motor unit population control tended to outperform single motor unit control. This may be attributed to the inherent nonlinear response characteristics of motor units, which make it difficult to control the firing rate of a specific motor unit to its maximum value over a long period of time[51]. Pooling multiple motor units together may average out these naturally occurring fluctuations, explaining the slightly improved control.

Limitations and future directions

Fatigue was a limiting factor for some participants, especially when maximal motor unit discharge rates were required. Similar to improving control accuracy, this challenge could be addressed by exploring the alternative mappings discussed earlier. Activating independent motor units simultaneously was slightly more difficult but is crucial for complex control. Besides asking participants to use more naturally occurring combinations of attempted movements, future work could explore whether more natural control signals could be formed from functionally defined motor unit populations[52], as a potential biologically grounded approach to improve multidimensional control.

Our work opens further promising avenues for future work. One involves sampling from more forearm and hand muscles, including intrinsic hand muscles, which may provide expanded control options. Future paradigms might also benefit from more intuitive mappings that simplify control, such as aligning cursor direction with anatomical movement patterns (for example, wrist flexion with the arm pronated moves the cursor downwards). Expanding the scope of application into real-world settings is an exciting opportunity, for example, by interfacing with consumer electronics.

Although outside the scope of this study, comparisons of motor unit control with standard assistive technologies, such as sip-and-puff systems or eye-tracking interfaces, and other approaches under development, such as BCIs, will also be needed for real-world translation. Given the challenges of performing extensive within-subject comparisons, this should probably involve benchmarking tasks and standardized metrics. Deployment for wider use will also require refinements on how motor-unit-based control signals are formed. These may include automated selection of optimal motor units for each attempted movement and how to combine these movements for multidimensional control. Although rare (~6% across all participants and sessions; Supplementary Fig. 2c), motor units could switch between being controllable and tonic; adaptive methods to classify motor units as such could be used to maintain controllability. Notably, the detection of single motor units might not be necessary in all users: P3's one-dimensional control with EMG was as good as with a population of motor units because his sparse EMG was very well correlated with the population activity (Supplementary Fig. 4a,b); an initial step to quantify the SNR of the EMG might help identify the necessity of decomposition.

We acknowledge that the sample in this study is small and heterogeneous, varying in age, clinical severity and duration of injury. That said, we are encouraged by the control accuracy our participants achieved despite prominent weakness and spasticity, which are common features in other neurological disorders such as stroke, neuropathy and myopathy. We would thus expect similar performance in people with other disorders that cause weakness if they have detectable motor units they can modulate. Finally, the fact that our approach of covering the proximal forearm with HDsEMG arrays and finding whichever units were controllable did not require specific tailoring to participant characteristics further makes it promising for other clinical populations.

Conclusion

This study provides evidence that individuals with lost hand function due to severe SCI can volitionally control the activity of motor units from paralysed muscles, which we detected with non-invasive EMG recordings. This control was rapidly acquired, accurate and multidimensional, and could be achieved despite the presence of complete paralysis and spasticity. While focusing on individuals with cervical SCI in this study, our approach may be applicable to other motor-impaired populations, including those affected by neuropathies, myopathies or stroke.

Methods

Participants

This study was approved by the National Health System Health Research Authority (REC reference 23/SW/0140) and Imperial College Research Ethics Committees (ICREC reference 19IC5641) and was performed in accordance with the Declaration of Helsinki.

Three male participants (P1, P2 and P3) who suffered from an SCI around the C1 to C4 level were included in this study. Each participant

provided written informed consent prior to participation. P1 is a male in his 30s who suffered a level C4 injury 24 months before the experiment. He was clinically classified as American Spinal Injury Association (ASIA) C (motor incomplete injury) and could generate no functional movements with his left hand and wrist (MRC power 0–1 in the hand and wrist), except for wrist extension. He had notable spasticity in his fingers and elbow, with fixed flexion at his metacarpophalangeal joint and elbow. P2 is a male in his 60s who suffered an SCI at the C1–C3 level 14 months prior to participating in this experiment. He was classified as ASIA C (incomplete tetraplegia) and had no movement in his right upper limb, rated MRC grade 0/5, except for a flicker of movement in his ring finger, rated MRC grade 1/5. His tone was flaccid in the upper limbs, and he had occasional myoclonic jerks of both arms and legs. P3 is a male in his 50s who sustained an SCI at the C2–C4 level 12 months prior to the experiment. He was classified as ASIA A (motor complete) and had no functional movement in either of his hands, with power rated at MRC grade 0–1/5 in the hand and wrist. His tone was spastic, and he had myoclonic jerks, although these were rare and mostly present in his lower limbs. All participants were deemed clinically stable by their treating clinician, defined as having no clinical change in the six months preceding recruitment to the study. The participant characteristics are summarized in Table 1.

Attempted movement screening and selection

In an initial calibration session, each participant was asked to attempt 16 movements (thumb flexion/extension/adduction/abduction, index flexion/extension, middle flexion/extension, ring flexion/extension, little flexion/extension and wrist flexion/extension/adduction/abduction) in turn while HDsEMG was recorded, and movement or flickers of movement were observed. We identified candidate attempted movements as those where HDsEMG was observable while there was minimal observable movement. We asked participants to select from these candidate movements going forward.

High-density EMG decomposition

We recorded HDsEMG signals using three 8 × 8 EMG grids (GR10MM0808, OT Bioelettronica) placed all around the forearm to cover all wrist and extrinsic hand muscles. The signals were recorded in a monopolar configuration (Quattrocento, OT Bioelettronica) using customized software, sampled at 2,048 Hz and band-pass filtered (10–500 Hz). Each experimental session included a calibration part and an online control part. During calibration, the participant was instructed to track a trapezoidal profile with a maximum of 100% (for P1) or 50% attempted maximum voluntary contraction (MVC) (for P2 and P3) using visual feedback on the global EMG amplitude. Then, a validated blind source separation algorithm was applied to decompose the recorded HDsEMG signals into constituent motor unit activity using these calibration data[25,26]. The detected motor units were retained when the silhouette (SIL) value was higher than 0.88; SIL is a clustering quality measure that reflects how well spike and noise centroids are separated after performing *K*-means clustering on extracted motor unit pulse trains. Manual editing was performed later to retain only high-quality motor units using standard approaches[53]. Duplicate motor units were detected by comparing their spike trains through cross-correlation. Each pair of motor unit spike trains was aligned across a ±50-ms lag range, and their similarity was measured as the fraction of spikes occurring within a ±5-ms coincidence window. Pairs showing more than 30% agreement were considered duplicates. For each duplicate set, the unit with the smallest inter-spike-interval coefficient of variation was kept. The identified motor unit filters for all the retained units were stored for later use for online visualization and control.

Online estimation of motor unit spiking events was achieved by applying the de-whitened stored motor unit filters to the incoming HDsEMG data[33,54]. The de-whitening procedure meant that the incoming EMG stream online need not be whitened, reducing processing latency. Spikes were identified by measuring the Euclidean distance between each pulse train value and the spike and noise centroids derived from offline decomposition for each motor unit. Values nearer to the spike centroid were labelled as spikes. This method removed the requirement for real-time *K*-means clustering and helped lower feedback latency. EMG signals were decomposed into constituent motor units in windows of 125 ms. Firing rates were calculated every 125 ms by counting the spikes detected over a 1,000-ms sliding window. We validated the accuracy of our online decomposition by comparing the motor unit action potential shapes (Supplementary Fig. 1a) and motor unit discharge times (Supplementary Fig. 1b) obtained through offline and online decomposition. In all cases, we observed a very good match.

Control signals

We compared the participants' ability to control the activity of single motor units, populations of motor units associated with the same attempted movement and the global surface EMG.

During calibration, the activity of individual motor units was displayed in real time using a raster plot. Participants attempted their selected movements, and a single motor unit was selected for individual motor unit control based on its controllability determined by the investigators and the participant. Motor units that were not activated during the attempted movement and motor units that fired tonically or indiscriminately during periods of contraction and rest were excluded. We averaged the firing rate of all the non-tonically firing motor units (that is, those under voluntary control) to form the motor unit population control signal. For control of the global surface EMG, bipolar EMG was first obtained by signal differencing along the muscle fibre direction; then, the overall EMG amplitude was calculated as the median root mean square (RMS) value of the EMG amplitudes across all channels from all grids.

All control signals were calculated in real time over a 1,000-ms window, sliding every 125 ms. That is, the 1,000-ms sliding window smoothed the controlled signals, which were updated every 125 ms. This smoothing window counteracted the inherent stochasticity of motor unit spiking behaviour; without it, cursor position could jump erratically on each 125-ms update, making control difficult irrespective of the participant's attempt. This choice thus trades temporal resolution (for fast corrections) with signal stability, to make volitional control tractable.

One-dimensional tracking tasks

We designed three distinct tracking profiles to evaluate the participants' ability to control their motor units subject to different task constraints, as well as to compare control signals (for example, Fig. 2b). These were:

(1) Trapezoidal profile: This profile increased linearly from 0 to the target MVC level within 6 s, remained constant for 15 s and then decreased linearly back to 0 within 6 s.
(2) Sinusoidal profile: This profile linearly ramped from 0 to the target MVC level within 6 s, oscillated around the target MVC level at an amplitude of ±20% of the target MVC level and a frequency of 0.25 Hz for 15 s and finally ramped linearly back to 0 within 6 s.
(3) Pseudosinusoidal profile: This profile consisted of four sinusoidal segments, each spanning two cycles and possessing a frequency of either 0.25 Hz or 0.5 Hz and an amplitude of either 50% or 100% of the target MVC level. The segments were randomly ordered (without repetition), phase-shifted backwards by one-quarter of a cycle and amplitude-shifted upwards to ensure non-negative values. This procedure produced a seamless final profile.

The target MVC level was 100% MVC for P1 and 50% MVC for P2 and P3. Participants performed three trials of each profile (trapezoidal,

sinusoidal and pseudosinusoidal) with each of the three control signals (single motor unit, motor unit population and EMG), resulting in a total of nine unique trial types and 27 trials per session. The order of these trials was randomized by assigning each combination of control signal and trial type a random number and sorting them accordingly. The tracking accuracy for each profile was quantified with the coefficient of determination (R^2). Participants completed four or five sessions of one-dimensional control.

The (residual) hand movements were recorded with a camera during the experiment to rule out the possibility that control was driven by flickers of motion (Supplementary Fig. 5).

Two-dimensional cursor navigation task

We next assessed whether participants could control a cursor in two dimensions using the activity of two independent motor units. We first stacked motor unit filters from two different movements to expand the dictionary of available motor units. Since each movement is performed separately, the offline HDsEMG per movement is associated with movement-specific whitening matrices. To account for statistical variability of the two different movements, a new whitening matrix derived from the concatenated EMG of the two different movements selected was calculated. This permitted recalibration of the spike and noise centroids necessary for stable online decomposition across both movements. Duplicate motor units across grids associated with the different movements were additionally removed, using the same spike-based threshold detailed under 'High-density EMG decomposition'.

Prior to the control experiments, we visualized the activity of all motor units using a real-time raster plot and screened for units that could be independently recruited. A motor unit was considered independent if it was selectively activated by one attempted movement without concurrent activation from the others. Once two motor units were confirmed to be independent, one was assigned to the cursor's position along the horizontal axis, and the other to the position along the vertical axis.

A two-dimensional cursor navigation task was designed to assess the control performance (Fig. 5a,b). Targets were distributed on the two-dimensional plane in a polar coordinate mode, with radial distances of 1/3, 2/3 and 1 of the maximum control range (defined as the average firing rate of each motor unit, calculated from the offline decomposition of the trapezoidal profile tracking), and angular positions of 0, $\pi/8$, $\pi/4$, $3\pi/8$ and $\pi/2$ rad, yielding a total of 16 targets. This 'rainbow' target distribution was designed to avoid two motor units being activated to their maximum discharge rates at the same time. Each target's position was randomly jittered within ±5% of the maximum control range of both axes to introduce additional spatial variability. The target size was ±15% of the maximum control range along the horizontal and vertical directions. In each session, participants were presented with all the targets in random order. A trial was considered successful if the participant acquired the target and held the cursor within it for at least 375 ms. The 375-ms holding period, corresponding to three consecutive 125-ms EMG processing windows, promoted intentional control, rather than quickly passing through the target bounds. Maximum trial duration was 15 s; the inter-trial time following a successful trial or a timed-out trial was 5 s, to allow for a rest period. In each two-dimensional control experiment, participants were asked to complete three blocks of trials of this task. Control performance was quantified on the basis of success rate, time to success and path efficiency, defined as the optimal path distance divided by the trial's path distance (for example, Fig. 5c,e). Expressed as a percentage, values of 100% mean a perfectly straight line to the target, whereas values tending towards 0% indicate increasingly meandering trajectories.

Three-bars task

Next, we expanded our approach for two-dimensional motor unit control to explore the feasibility of controlling three independent motor units. Similar to two-dimensional control, we sought to identify an additional independent motor unit by decomposing HDsEMG signals from a third attempted movement. To validate the participant's ability to independently control the three motor units, we first performed the two-dimensional cursor navigation task using pairwise combinations of the three motor units, restricting the targets to the horizontal and vertical axes and excluding diagonal targets (Fig. 6a).

In addition to this pairwise assessment, we designed a 'three bars' task to more directly evaluate three-dimensional control. In this task, three targets were assigned to each motor unit, corresponding to 1/3, 2/3 and its full maximum firing rate, respectively. Here, the maximum firing rate was defined as the average firing rate calculated from the offline decomposition of the trapezoidal profile tracking. Target size was again defined as ±15% of the maximum firing rate. We designed two versions of this task: one to probe independent control and the other to probe simultaneous control. The independent control version of the task had nine conditions; in each condition, one motor unit was assigned to one of the three contraction levels while the other two remained quiescent (Fig. 6b). The participants were asked to complete three blocks of this task during a single session. The simultaneous control version of the task required not only individuation of single motor units but also the co-activation of motor unit pairs. Three targets were assigned to each motor unit, corresponding to 0, 1/2 and the full maximum firing rate. Only co-activation with 1/2 the maximum firing rate was considered to avoid simultaneous activation of multiple motor units to the maximum level. This led to 11 task conditions (Fig. 6d); participants were asked to complete one block of this co-activation bar task in one session. Control performance was also quantified based on success rate and time to success.

Pong, Snake and virtual wheelchair control

To expand control outside of constrained laboratory tasks designed to probe performance and generalization, we built virtual environments for participants to play adapted versions of Pong and Snake and to control a virtual wheelchair.

In Pong[31], participants controlled the vertical position of a paddle (1/5 of the game window's height) to intercept a ball bouncing within the screen's boundaries (Fig. 7a). The paddle's vertical position was mapped linearly in real time to the firing rate of a selected motor unit or a population of motor units, such that higher firing rates produced greater upward displacement. This position was updated every 125 ms. Ball trajectories were semi-randomized and followed the law of reflection: each reset positioned the ball at the centre with a trajectory directed away from the paddle. The selected attempted movements for each participant were the same as those in the one-dimensional tracking.

In Snake[32], participants used two motor units to control 90° clockwise and 90° counterclockwise rotations of a virtual snake within an 80 × 80 grid (Fig. 7b). The selected attempted movements for each participant were the same as those in the two-dimensional cursor navigation. The snake moved one step forwards every 330 ms, and participants could update the control commands every 125 ms. Participants had to select the correct motor unit at the right time to direct the snake towards food (red box), which appeared at random locations in the workspace. Once the snake entered the food area (with a tolerance of ±1 grid unit), the food was eaten, resulting in the snake's overall length increasing by one. A trial was deemed to have failed if the snake intercepted itself (rather than food); if the snake reached the end of the screen, it reappeared at the opposite side.

We rerouted the activity of three independent motor units that allowed P1 to drive a virtual wheelchair developed in Unity (Unity Technologies) (Fig. 7c). He controlled the forward drive, left turn and right turn of the wheelchair using thumb adduction, wrist abduction and wrist flexion. The wheelchair moved one step every 125 ms. P1 controlled the forward movement by continuously activating the thumb adduction motor unit. The velocity of the wheelchair was proportional

to the activation level of the motor unit. Discrete 90° clockwise and counterclockwise turns were achieved by activating the wrist abduction or wrist flexion motor units.

Additional analyses

(1) Offline validation of online motor unit decomposition (Supplementary Fig. 1a,b): To validate the accuracy of the online motor unit decomposition algorithm beyond the ability of the participants to control these detected motor units, we compared the motor unit action potentials and motor unit spike trains obtained from the online experiment with those from offline re-decomposition (that is, offline decomposition of online recordings). Pearson's correlation coefficient and the rate of agreement were used to assess the correlation between motor unit action potentials and the consistency of motor unit spike trains between motor unit activity tracked online and verified offline, respectively.

(2) Quantifying the proportion of controllable units that become tonic (Supplementary Fig. 2b,c): We observed that some controllable motor units became tonic after tracking a target profile. We characterized the occurrence of this phenomenon by calculating the proportion of motor units that became tonic at the beginning of the next trial.

(3) Relationship between the global EMG and decomposed motor unit population activity (Supplementary Fig. 4a,b): To understand the relationship between the global EMG and the activity of the detected motor unit population, we calculated the Pearson's correlation coefficient between the EMG RMS and the firing rate of the motor unit population during the trials in which participants tracked the different profiles using the global EMG. The motor unit activity was decomposed from the offline recorded HDsEMG using a pseudo-online mode, by applying the calibrated motor unit filters and parameters used during the online experiments. In addition, the EMG SNR was calculated to help elucidate the relationship between EMG 'quality' and the activity from the detected motor unit population (Supplementary Fig. 4c). The SNR was defined as the ratio of the RMS value of the global EMG signal during MVC to the RMS value of baseline global EMG noise as $\mathrm{SNR} = 20\log_{10}\frac{\mathrm{RMS}(\mathrm{EMG}_{\mathrm{mvc}})}{\mathrm{RMS}(\mathrm{EMG}_{\mathrm{baseline}})}$.

(4) Simulations of one-dimensional profile tracking without exclusion of tonically active motor units (Supplementary Fig. 4d): To illustrate the effect of tonic motor unit activity on the control signal, we reapplied the motor unit filters to the HDsEMG data recorded during one-dimensional profile tracking, this time without excluding tonic units, to reconstruct offline the control signal that would have resulted from including tonic alongside controllable units. This reflects the raw effect of tonic motor unit activity on the control signal rather than a true simulation of online control, which would also involve patient compensation via visual feedback.

(5) Relationship between attempted residual movements and motor unit activity (Supplementary Fig. 5): To quantify the relationship between motor unit population activity and the residual hand kinematics, we extracted hand kinematics from the recorded videos during the one-dimensional tracking tasks (Fig. 2). First, the videos were cropped to hand-view frames and converted to greyscale. Subsequently, we performed a principal component analysis of the changes in image pixel values; we considered the first principal component as an indicator of attempted movement. Finally, we measured the similarity between the inferred kinematics and the motor unit population activity as their coefficient of determination (R^2).

(6) Compensation of control delays for pseudosinusoidal tracking (Supplementary Fig. 6a): During the pseudosinusoidal profile tracking, we noticed that participants could usually track the amplitude well but with an apparent time delay. To better measure the quality of amplitude control and the temporal precision of the control, we segmented the full profile into eight semi-sinusoidal segments and then calculated the tracking accuracy after aligning the online profile to each segment using cross-correlation. The tracking accuracy after alignment and the estimated time delay with cross-correlation were then used to better characterize the pseudosinusoidal control.

(7) Quantification of the strategies used during two-dimensional control (Supplementary Fig. 8): We noted that participants used two strategies, to varying degrees, during the two-dimensional control task: they either simultaneously activated two motor units or activated one motor unit followed by the other. We quantified how much each of these strategies was used during each two-dimensional control trial using two metrics termed co-activation ratio and individual activation ratio. We considered a motor unit to be active when its firing rate was above zero. For each trial, we calculated the amount of time that both units were active and expressed this as a proportion of the trial's total time, resulting in the co-activation ratio. Individual activation was calculated in a similar fashion, except for instances where one motor unit was active while the other stayed silent. Notably, they are not one minus the other: instances where both units did not fire are not counted in either ratio.

Statistics

Data were collected and analysed using MATLAB R2024b (MathWorks Inc.) and IBM SPSS Statistics version 26. Each session (one day of the experiment) comprised multiple trials, where a trial denotes tracking one profile or one repetition of a multidimensional control task. Performance within a session was quantified by aggregating across trials, and the effect of practice was assessed by comparing performance across sessions. The number of participants in this case series was not large enough for a robust inter-user statistical analysis, considering the large clinical diversity; therefore, results are reported for each participant individually.

To quantify whether continued practice improved one-dimensional motor unit control, we fitted within-participant linear regression models using the fitlm function. The sign of the fitting slope (β) was used to evaluate the effect of practice on control performance, and the P value, the statistical significance of the linear fit. P values were computed from the t-statistic, which assessed whether the slope (β) of the regression line was significantly different from zero[55]. To compare the performance for trained and untrained movements during the two-dimensional navigation tasks, we first used a modified version of the Kolmogorov–Smirnov test after testing for normality using the lillietest function. If the data met the normality assumption, we used a parametric independent-sample two-sided t-test to assess statistical significance; otherwise, we used a nonparametric two-sided Mann–Whitney U-test. This comparison was done within-participant by comparing performance across different trials. The statistical significance level was set to 0.05.

Reporting summary

Further information on research design is available in the Nature Portfolio Reporting Summary linked to this article.

Data availability

Data will be available upon request after signature of a materials transfer agreement.

Code availability

All the analysis code is available via Zenodo at https://doi.org/10.5281/zenodo.22177904 (ref. 56).

References

1. Safdarian, M. et al. Global, regional, and national burden of spinal cord injury, 1990–2019: a systematic analysis for the Global Burden of Disease Study 2019. *Lancet Neurol.* **22**, 1026–1047 (2023).
2. Anderson, K. D. Targeting recovery: priorities of the spinal cord-injured population. *J. Neurotrauma* **21**, 1371–1383 (2004).
3. Barra, B. et al. Epidural electrical stimulation of the cervical dorsal roots restores voluntary upper limb control in paralyzed monkeys. *Nat. Neurosci.* **25**, 924–934 (2022).
4. Badi, M. et al. Intrafascicular peripheral nerve stimulation produces fine functional hand movements in primates. *Sci. Transl. Med.* **13**, eabg6463 (2021).
5. Ajiboye, A. B. et al. Restoration of reaching and grasping movements through brain-controlled muscle stimulation in a person with tetraplegia: a proof-of-concept demonstration. *Lancet* **389**, 1821–1830 (2017).
6. Bouton, C. E. et al. Restoring cortical control of functional movement in a human with quadriplegia. *Nature* **533**, 247–250 (2016).
7. Ethier, C., Oby, E. R., Bauman, M. J. & Miller, L. E. Restoration of grasp following paralysis through brain-controlled stimulation of muscles. *Nature* **485**, 368–371 (2012).
8. Hochberg, L. R. et al. Neuronal ensemble control of prosthetic devices by a human with tetraplegia. *Nature* **442**, 164–171 (2006).
9. Collinger, J. L. et al. High-performance neuroprosthetic control by an individual with tetraplegia. *Lancet* **381**, 557–564 (2013).
10. Willett, F. R., Avansino, D. T., Hochberg, L. R., Henderson, J. M. & Shenoy, K. V. High-performance brain-to-text communication via handwriting. *Nature* **593**, 249–254 https://doi.org/10.1038/s41586-021-03506-2 (2021).
11. Dalrymple, A. N., Jones, S. T., Fallon, J. B., Shepherd, R. K. & Weber, D. J. Overcoming failure: improving acceptance and success of implanted neural interfaces. *Bioelectron. Med.* **11**, 6 (2025).
12. Balbinot, G. et al. Segmental motor recovery after cervical spinal cord injury relates to density and integrity of corticospinal tract projections. *Nat. Commun.* **14**, 723 (2023).
13. Oliveira, D. S. et al. A direct spinal cord–computer interface enables the control of the paralysed hand in spinal cord injury. *Brain* **147**, 3583–3595 (2024).
14. Ting, J. E. et al. Sensing and decoding the neural drive to paralyzed muscles during attempted movements of a person with tetraplegia using a sleeve array. *J. Neurophysiol.* **126**, 2104–2118 (2021).
15. Sîmpetru, R. C. et al. MyoGestic: EMG interfacing framework for decoding multiple spared motor dimensions in individuals with neural lesions. *Sci. Adv.* **11**, eads9150 (2025).
16. Lu, Z., Stampas, A., Francisco, G. E. & Zhou, P. Offline and online myoelectric pattern recognition analysis and real-time control of a robotic hand after spinal cord injury. *J. Neural Eng.* **16**, 036018 (2019).
17. Yun, Y. et al. Maestro: an EMG-driven assistive hand exoskeleton for spinal cord injury patients. In *2017 IEEE International Conference on Robotics and Automation* 2904–2910 (IEEE, 2017).
18. Balbinot, G. et al. Properties of the surface electromyogram following traumatic spinal cord injury: a scoping review. *J. Neuroeng. Rehabil.* **18**, 105 (2021).
19. Sköld, C., Levi, R. & Seiger, Å. Spasticity after traumatic spinal cord injury: nature, severity, and location. *Arch. Phys. Med. Rehabil.* **80**, 1548–1557 (1999).
20. Maynard, F., Karunas, R. & Waring, W.3rd. Epidemiology of spasticity following traumatic spinal cord injury. *Arch. Phys. Med. Rehabil.* **71**, 566–569 (1990).
21. Gorassini, M. A., Knash, M. E., Harvey, P. J., Bennett, D. J. & Yang, J. F. Role of motoneurons in the generation of muscle spasms after spinal cord injury. *Brain* **127**, 2247–2258 (2004).
22. Zijdewind, I. & Thomas, C. K. Spontaneous motor unit behavior in human thenar muscles after spinal cord injury. *Muscle Nerve* **24**, 952–962 (2001).
23. Souza de Oliveira, D. et al. Spared motor neurons enable control of a robotic sixth finger for functional grasping in tetraplegia. *IEEE Trans. Neural Syst. Rehabil. Eng.* **34**, 4042–4051 (2026).
24. Yang, X. et al. Non-invasive neural interfacing for tetraplegic individuals using residual motor neuron activity decoded at the forearm or wrist. *IEEE J. Biomed. Health Inform.* **29**, 7140–7148 (2025).
25. Holobar, A. & Zazula, D. Multichannel blind source separation using convolution kernel compensation. *IEEE Trans. Signal Process.* **55**, 4487–4496 (2007).
26. Negro, F., Muceli, S., Castronovo, A. M., Holobar, A. & Farina, D. Multi-channel intramuscular and surface EMG decomposition by convolutive blind source separation. *J. Neural Eng.* **13**, 026027 https://doi.org/10.1088/1741-2560/13/2/026027 (2016).
27. Murray, K. C. et al. Recovery of motoneuron and locomotor function after spinal cord injury depends on constitutive activity in 5-HT2C receptors. *Nat. Med.* **16**, 694–700 (2010).
28. Zijdewind, I. & Thomas, C. K. Firing patterns of spontaneously active motor units in spinal cord-injured subjects. *J. Physiol.* **590**, 1683–1697 (2012).
29. Farina, D. & Negro, F. Common synaptic input to motor neurons, motor unit synchronization, and force control. *Exerc. Sport Sci. Rev.* **43**, 23–33 (2015).
30. Farina, D., Negro, F. & Dideriksen, J. L. The effective neural drive to muscles is the common synaptic input to motor neurons. *J. Physiol.* **592**, 3427–3441 (2014).
31. Wikipedia contributors. Pong https://en.wikipedia.org/w/index.php?title=Pong&oldid=1323327675 (2025).
32. Wikipedia contributors. Snake (1998 video game) https://en.wikipedia.org/w/index.php?title=Snake_(1998_video_game)&oldid=1317837783 (2025).
33. Rossato, J. et al. I-Spin live, an open-source software based on blind-source separation for real-time decoding of motor unit activity in humans. *eLife* **12**, RP88670 (2024).
34. Hutson, T. H. & Di Giovanni, S. The translational landscape in spinal cord injury: focus on neuroplasticity and regeneration. *Nat. Rev. Neurol.* **15**, 732–745 (2019).
35. Lin, D. J., Cramer, S. C., Boyne, P., Khatri, P. & Krakauer, J. W. High-dose, high intensity stroke rehabilitation: why aren't we giving it? *Stroke* **56**, 1351–1364 (2025).
36. Dawson, A. et al. High-dose high-intensity arm neurorehabilitation in chronic stroke improves general motor control. Preprint at *medRxiv* https://doi.org/10.1101/2025.11.18.25340491 (2025).
37. Makin, T. R. & Krakauer, J. W. Against cortical reorganisation. *eLife* **12**, e84716 (2023).
38. Edelman, B. J. et al. Noninvasive neuroimaging enhances continuous neural tracking for robotic device control. *Sci. Robot.* **4**, eaaw6844 (2019).
39. Lee, J. Y. et al. Brain–computer interface control with artificial intelligence copilots. *Nat. Mach. Intell.* **7**, 1510–1523 (2025).
40. Hwang, H.-J., Kwon, K. & Im, C.-H. Neurofeedback-based motor imagery training for brain–computer interface (BCI). *J. Neurosci. Methods* **179**, 150–156 (2009).
41. Ghavampour, A. et al. A paradigm to study the learning of muscle activity patterns outside of the natural repertoire. *J. Neurophysiol.* **134**, 347–360 (2025).
42. Sadtler, P. T. et al. Neural constraints on learning. *Nature* **512**, 423–426 (2014).

43. Willsey, M. S. et al. A high-performance brain–computer interface for finger decoding and quadcopter game control in an individual with paralysis. *Nat. Med.* **31**, 96–104 (2025).
44. Carmena, J. M. et al. Learning to control a brain–machine interface for reaching and grasping by primates. *PLoS Biol.* **1**, e42 (2003).
45. Li, D., Chen, C., Zhu, K., Guo, R. & Shull, P. B. Integrating motor unit activity with deep learning for real-time, simultaneous and proportional wrist angle and grasp force estimation. *IEEE Trans. Biomed. Eng.* **72**, 3682–3693 (2025).
46. Schone, H. R. et al. Biomimetic versus arbitrary motor control strategies for bionic hand skill learning. *Nat. Hum. Behav.* **8**, 1108–1123 (2024).
47. Farina, D., Merletti, R. & Enoka, R. M. The extraction of neural strategies from the surface EMG. *J. Appl. Physiol.* **96**, 1486–1495 (2004).
48. Day, S. *Important Factors in Surface EMG Measurement* (Bortec Biomedical Ltd, 2002).
49. Farina, D., Mesin, L., Martina, S. & Merletti, R. A surface EMG generation model with multilayer cylindrical description of the volume conductor. *IEEE Trans. Biomed. Eng.* **51**, 415–426 (2004).
50. Braun, D. I. et al. NeurOne: High-performance motor unit–computer interface for the paralyzed. Preprint at *medRxiv* https://doi.org/10.1101/2023.09.25.23295902 (2023).
51. Fuglevand, A. J., Lester, R. A. & Johns, R. K. Distinguishing intrinsic from extrinsic factors underlying firing rate saturation in human motor units. *J. Neurophysiol.* **113**, 1310–1322 (2015).
52. Hug, F., Avrillon, S., Ibáñez, J. & Farina, D. Common synaptic input, synergies and size principle: control of spinal motor neurons for movement generation. *J. Physiol.* **601**, 11–20 (2023).
53. Del Vecchio, A. et al. Tutorial: analysis of motor unit discharge characteristics from high-density surface EMG signals. *J. Electromyogr. Kinesiol.* **53**, 102426 (2020).
54. Barsakcioglu, D. Y., Bräcklein, M., Holobar, A. & Farina, D. Control of spinal motoneurons by feedback from a non-invasive real-time interface. *IEEE Trans. Biomed. Eng.* **68**, 926–935 (2020).
55. Montgomery, D. C., Peck, E. A. & Vining, G. G. *Introduction to Linear Regression Analysis* (John Wiley & Sons, 2021).
56. Yang, X., Rawji, V., Gibbs, C., Farina, D. & Gallego, J. Á. Code scripts accompanying manuscript titled: 'Intuitive, multidimensional motor unit control after paralysing spinal cord injury using non-invasive recordings'. *Zenodo* https://doi.org/10.5281/zenodo.22177903 (2025).

Acknowledgements

We thank our participants and their carers for their time, patience and efforts. We also thank the Alderbourne and Daniels Rehabilitation Unit at Hillingdon Hospital, including the clinicians, nurses and therapy staff for their assistance in identifying participants and providing us with the environment to conduct this study. Finally, we also thank S. Avrillon for providing technical support and open-source software during the early stages of the project, B. Hodossy for contributing the virtual wheelchair environment and C. Massumoto for her help with figure editing.

Author contributions

X.Y., V.R., C.G., D.F. and J.A.G. designed the study. V.R. and A.N. recruited the participants. X.Y., V.R. and C.G. collected the data with help from T.J., L.G.V. and A.G. in specific sessions. X.Y. provided the main software. X.Y., V.R., C.G., D.F. and J.A.G. devised the analyses, and X.Y. implemented them. X.Y., V.R., C.G., D.F. and J.A.G. wrote the manuscript.

Funding

X.Y. is supported by the Fundamental Research Funds for the Central Universities, grant no. 2242025F20002. V.R. is supported by an NIHR Academic Clinical Fellowship. C.G. is supported by the Imperial College London President's PhD Scholarship. This work was supported by the Imperial-META Wearable Neural Interfaces Research Centre (D.F. and J.A.G.), grant no. EP/T020970/1 from the UKRI Engineering and Physical Sciences Research Council (D.F. and J.A.G.) and grant no. ERC-2020-StG-949660 from the European Research Council (J.A.G.). The funders had no role in study design, data collection and analysis, decision to publish or preparation of the manuscript.

Competing interests

D.F. receives research funding from Meta Platform Technologies. J.A.G. receives research funding from Meta Platform Technologies and InBrain Neuroelectronics. The other authors declare no competing interests.

Additional information

Supplementary information The online version contains supplementary material available at https://doi.org/10.1038/s41562-026-02626-x.

Correspondence and requests for materials should be addressed to Dario Farina or Juan Alvaro Gallego.

Peer review information *Nature Human Behaviour* thanks Enzo Mastinu, Silvestro Micera, Argyrios Stampas and the other, anonymous, reviewer(s) for their contribution to the peer review of this work. Peer reviewer reports are available.

Reprints and permissions information is available at www.nature.com/reprints.

Publisher's note Springer Nature remains neutral with regard to jurisdictional claims in published maps and institutional affiliations.

Open Access This article is licensed under a Creative Commons Attribution 4.0 International License, which permits use, sharing, adaptation, distribution and reproduction in any medium or format, as long as you give appropriate credit to the original author(s) and the source, provide a link to the Creative Commons licence, and indicate if changes were made. The images or other third party material in this article are included in the article's Creative Commons licence, unless indicated otherwise in a credit line to the material. If material is not included in the article's Creative Commons licence and your intended use is not permitted by statutory regulation or exceeds the permitted use, you will need to obtain permission directly from the copyright holder. To view a copy of this licence, visit http://creativecommons.org/licenses/by/4.0/.

© The Author(s) 2026

nature portfolio

Corresponding author(s): Dario Farina, Juan A Gallego

Last updated by author(s): Aug 19, 2026

Reporting Summary

Nature Portfolio wishes to improve the reproducibility of the work that we publish. This form provides structure for consistency and transparency in reporting. For further information on Nature Portfolio policies, see our Editorial Policies and the Editorial Policy Checklist.

Statistics

For all statistical analyses, confirm that the following items are present in the figure legend, table legend, main text, or Methods section.

n/a	Confirmed	
☐	☒	The exact sample size (*n*) for each experimental group/condition, given as a discrete number and unit of measurement
☐	☒	A statement on whether measurements were taken from distinct samples or whether the same sample was measured repeatedly
☐	☒	The statistical test(s) used AND whether they are one- or two-sided *Only common tests should be described solely by name; describe more complex techniques in the Methods section.*
☒	☐	A description of all covariates tested
☒	☐	A description of any assumptions or corrections, such as tests of normality and adjustment for multiple comparisons
☐	☒	A full description of the statistical parameters including central tendency (e.g. means) or other basic estimates (e.g. regression coefficient) AND variation (e.g. standard deviation) or associated estimates of uncertainty (e.g. confidence intervals)
☐	☒	For null hypothesis testing, the test statistic (e.g. *F*, *t*, *r*) with confidence intervals, effect sizes, degrees of freedom and *P* value noted *Give P values as exact values whenever suitable.*
☒	☐	For Bayesian analysis, information on the choice of priors and Markov chain Monte Carlo settings
☒	☐	For hierarchical and complex designs, identification of the appropriate level for tests and full reporting of outcomes
☐	☒	Estimates of effect sizes (e.g. Cohen's *d*, Pearson's *r*), indicating how they were calculated

Our web collection on statistics for biologists contains articles on many of the points above.

Software and code

Policy information about availability of computer code

Data collection	EMG data was aquired using a commercially available high-density EMG system (Quattrocento, OT Bioelettronica), using a customized MATLAB software (see below). To isolate the activity of single motor units for online control, we used a validated blind source separation method (available at Rossato et al, eLife, 2024). We also recorded movies of the arm to assess micromovements.
Data analysis	The data were collected and analysed using MATLAB R2024b (MathWorks Inc.) using standard methods in the field. EMG decomposition code is publicly available (Rossato et al, eLife, 2024). Some additional analyses were conducted on IBM SPSS Statistics 26.

For manuscripts utilizing custom algorithms or software that are central to the research but not yet described in published literature, software must be made available to editors and reviewers. We strongly encourage code deposition in a community repository (e.g. GitHub). See the Nature Portfolio guidelines for submitting code & software for further information.

Data

Policy information about availability of data

All manuscripts must include a data availability statement. This statement should provide the following information, where applicable:

- Accession codes, unique identifiers, or web links for publicly available datasets
- A description of any restrictions on data availability
- For clinical datasets or third party data, please ensure that the statement adheres to our policy

Videos can be found on Zenodo (https://doi.org/10.5281/zenodo.17841392) and have been uploaded with the manuscript. Data will be made available upon reasonable request to the corresponding author (they have not yet been appropriately curated for public distribution).

Research involving human participants, their data, or biological material

Policy information about studies with human participants or human data. See also policy information about sex, gender (identity/presentation), and sexual orientation and race, ethnicity and racism.

Reporting on sex and gender	The sex of each participant has been included in the Methods section. We included three male participants.
Reporting on race, ethnicity, or other socially relevant groupings	We have not included the race, ethnicity nor socially relevant groups of the participants in this study as we believe they bear no influence of the outcomes of this study.
Population characteristics	We have included the age, level and duration of spinal cord injury, and the amount of residual function. These characteristics serve to contextualise our findings.
Recruitment	Participants were recruited via spinal cord injury charities and patient groups in the United Kingdom. They have been credited in our Acknowledgments section. Participants were selected based on their suitability according to clinical characteristics.
Ethics oversight	Ethical approval was provided by the NHS HRA (REC reference 23/SW/0140) and Imperial College Research Ethics Committees (ICREC reference 19IC5641), and was performed in accordance with the Declaration of Helsinki.

Note that full information on the approval of the study protocol must also be provided in the manuscript.

Field-specific reporting

Please select the one below that is the best fit for your research. If you are not sure, read the appropriate sections before making your selection.

☒ Life sciences ☐ Behavioural & social sciences ☐ Ecological, evolutionary & environmental sciences

For a reference copy of the document with all sections, see nature.com/documents/nr-reporting-summary-flat.pdf

Life sciences study design

All studies must disclose on these points even when the disclosure is negative.

Sample size	Three participants (all male, in their thirties, fifties and sixties, respectively) with no residual function of the hand following a spinal cord injury (MRC scale, 0-1) were chosen to undergo the study protocol, including repeated experimental sessions to test performance gains and explore the dimensionality of the control space. The selected participants were clinically distinct (e.g., in terms of sensory deficit) to guarantee, as much as possible, reproducibility beyond the scope of this proof-of-principle study. Our selection criteria and demands of the study, detailed in the paper, also meant that few of those screened were eligible.
Data exclusions	No data were excluded from analyses.
Replication	The main findings of one-dimensional control with multiple muscle signals over multiple sessions, and two-dimesional cursor control were replicated in all three participants. Two participants performed our three-dimensional control experiments, to replicate this core result. None of those results failed to generalize. Finally, different participants engaged with different games and functional tasks to show proof of concept for follow up studies.
Randomization	There were no experimental groups and hence randomisation was not required.
Blinding	There were no treatment groups so blinding was not relevant.

Reporting for specific materials, systems and methods

We require information from authors about some types of materials, experimental systems and methods used in many studies. Here, indicate whether each material, system or method listed is relevant to your study. If you are not sure if a list item applies to your research, read the appropriate section before selecting a response.

Materials & experimental systems

n/a	Involved in the study
☒	☐ Antibodies
☒	☐ Eukaryotic cell lines
☒	☐ Palaeontology and archaeology
☒	☐ Animals and other organisms
☒	☐ Clinical data
☒	☐ Dual use research of concern
☒	☐ Plants

Methods

n/a	Involved in the study
☒	☐ ChIP-seq
☒	☐ Flow cytometry
☒	☐ MRI-based neuroimaging

Plants

Seed stocks	n.a.
Novel plant genotypes	n.a.
Authentication	n.a.